Dysregulated expression of mRNA and SNP in pulmonary artery remodeling in ascites syndrome in broilers

Sufang Cheng,[†,1] Xin Liu,[§,1] Pei Liu,[*] Guyue Li,[*] Xiaoquan Guo,[*] Guoliang Hu,[*] Lin Li,[*] Cong Wu,[*] Zheng Xu,[‡] Qi Zhou,[*] Jialin Jiang,[†] Shixian Luo,[#] Huajun Huang,[*] and Ping Liu[*,2]

*Jiangxi Provincial Key Laboratory for Animal Health, Institute of Animal Population Health, College of Animal Science and Technology, School of Land Resources and Environment, Key Laboratory of Agricultural Resource and Ecology in the Poyang Lake Basin of Jiangxi Province, Jiangxi Agricultural University, Nanchang 330045, PR China; †Department of Animal Science, Jiangxi Biological Vocational College, Nanchang, Jiangxi 330200, China; ‡Department of Mathematics and Statistics, Wright State University, Dayton, OH, 45435; §Department of Animal Science, Jiangxi Taihe Lvsejunong Agriculture and Animal Husbandry Food Co., Ltd., Taihe, Jiangxi 343700, China; and #Department of Animal Science, Animal Husbandry and Veterinary Bureau of Taihe, Taihe, Jiangxi 343700, China

ABSTRACT Broiler ascites syndrome (**AS**), also called pulmonary artery hypertension, is a metabolic disorder that has been observed worldwide in fast-growing broilers. Pulmonary arterial remodeling is a key step in the development of AS. The precise relationship between mRNA and SNP of the pulmonary artery in regulating AS progression remains unclear. In this study, we obtained pulmonary artery tissues from broilers with AS to perform pathologic section and pathologic anatomic observation. SNP, InDel, and mRNA data analysis were carried out using GATK and ANNOVAR software to study the SNP loci of 985 previously reported genes (437 upregulated and 458 downregulated). The pathology results showed that there was a lot of yellow fluid in the abdominal cavity and pericardium, that the ascites cardiac index and hematocrit changed significantly, and that the pulmonary artery had remodeled and become thicker in the disease group. Myocardial sections showed vacuolar degeneration of myocytes and rupture of muscle fibers. In addition, ALDH7A1, IRG1, GGT5, IGSF1, DHX58, USP36, TREML2, SPAG1, CD34, and PLEKHA7 were found to be closely associated with the pathogenesis of pulmonary artery remodeling in AS progression. Taken together, our present study further illuminates the molecular mechanism of pulmonary artery remodeling underlying AS progression.

Key words: ascites syndrome of broiler, pulmonary artery remodeling, mRNA, SNP

INTRODUCTION

Pulmonary arterial hypertension (**PAH**), also called pulmonary hypertension (**PH**) or broiler ascites syndrome (**AS**), is a metabolic disorder disease, which has been observed worldwide in fast growing broilers. It is characterized of excess proliferation, apoptosis resistance, inflammation, fibrosis, and vasoconstriction. Many researchers believe that AS is related to nutritional, management, environmental, and genetic factors (Julian, 2000; Olkowski, 2007; Baghbanzadeh and Decuypere, 2008). Ascites syndrome could cause relative hypoxia in the chicken's body, resulting in a series of pathophysiological changes including PH, pulmonary vascular remodeling, and cardiac hypertrophy and failure, the production of free radicals which could increase lipid peroxidation, and so on (Wideman et al., 2013). Recent studies have found the impact of pulmonary vascular remodeling on the development of PAH which involves a complex and multifactorial process in which endothelium-derived vasoactive molecules, such as endothelin-1, vascular endothelial growth factor, insulin-like growth factors-II, transforming growth factor-α, platelet-derived growth factor receptor, erythropoietin, and hypoxia-inducible factor-la (HIF-lα) (Schermuly et al., 2011; Papamatheakis et al., 2013; Shimoda and Laurie, 2013; Wideman et al., 2013). These

molecules have been increasingly recognized as critical factors and potential therapeutic targets in the treatment of PAH. In addition, these protein-coding genes contain at least 1 conserved microRNAs (**miRNA**)-binding site and numerous nonconserved site; most protein-coding genes may be under the control of miRNA (Schermuly et al., 2011; Papamatheakis et al., 2013; Shimoda and Laurie, 2013; Wideman et al., 2013). However, SNP within target genes could alter miRNA expression owing to altered mRNA levels. Thus, it has also been proposed that SNP within miRNA target genes (**mRNA**) that are associated with disease risk could be operating through their influence on miRNA (Mullany et al., 2015).

Currently, this study provides a unique position to assess whether the SNP gene loci and target genes of miRNA influence miRNA expression in PAH underlying AS in broilers. To determine whether some SNP alter miRNA expression levels, we used non-PAH tissue and PAH tissue to evaluated the differences in the expression across genotypes. However, because an SNP could alter miRNA expression levels equally in both PAH and non-PAH tissue, such an association would not necessarily contribute to PAH underlying AS in broilers' risk. To determine whether SNP are associated with PAH by miRNA regulation, we sought to understanding the regulatory mechanism of miRNA and SNP related to target genes for altering the remodeling phenotype in the pulmonary vasculature. Finally, we evaluated the SNP associated with miRNA expression and the risk of PAH underlying AS in broilers.

MATERIALS AND METHODS

Ethics Statement, Experimental Design, and Animal Management

All animal experiments were approved by the Institutional Animal Care and Use Committee of Jiangxi Agricultural University. All care and procedures of the broiler chickens were made in strict accordance with the Guidelines of the Institutional Animal Care and Use Committee of Jiangxi Agricultural University. All efforts were carried out to minimize the suffering of the animals. Seventy five 21-day-old male Arbor Acre commercial broiler chickens were randomly divided into 2 groups: the normal group (20 birds) and the disease group (55 birds). All broilers in the normal group were put in the room temperature ($20°C–25°C$) and provided with tap water, while the broilers in the disease group were put in a relatively low temperature (approximately $14°C$) and provided with the water with 0.3% salt. All birds were allowed to have free access to the same diet.

Sample Collection and Preparation

At the syndrome peak (35 d of age) from 28 d of age to 42 d of age, we paid close attention to the birds and the suspicious AS-like symptoms such as reluctance to move, AS-like depression, open-beak breathing, distended abdomen, and cyanosis. Once the birds were going to die, they were immediately sampled. At the time of necropsy, venous blood samples were taken from the wings to perform complete blood count. After removing the atrium and aorta, the right ventricle was separated from the septum and the left ventricular to measure ascites heart index (**AHI**), and then, right ventricular and total ventricular were weighted. In the meantime, the pulmonary artery was collected and quickly rinsed in the saline water. A part of the pulmonary artery was quickly frozen in liquid nitrogen and then stored in a refrigerator at $-80°C$ for RNA sequencing, while another part of the pulmonary artery was cut and stored in 10% formaldehyde for pathologic observation. The samples were selected for the transcriptomic profile analysis based on the AS judgment criteria including AHI, hematocrit (**HCT**) and presence of yellow liquid in abdominal cavity and pericardium. Birds with AS were selected from the AS group (AHI > 0.28; HCT > 36%; presence of yellow liquid in abdominal cavity and pericardium) (Julian et al., 2000; Liu et al., 2017; Mullany et al., 2015). Normal chickens were selected from the normal group (AHI <0.219; HCT < 28%; presence of free yellow liquid in abdominal cavity and pericardium).

Histopathologic Examination of the Pulmonary Artery

To evaluate the histopathologic changes in the pulmonary arteries of broilers with AS, pulmonary arteries previously stored in 10% formaldehyde were transferred into 4% paraformaldehyde for more than 24 h to thoroughly fix the structure of the tissue. Then, pulmonary artery tissues were put in an ascending gradient of ethanol (70–99.5%) for dehydration. They were made transparent by dipping in xylene 3 times (for 4 min, 2 min, and 30 s). Next, they were put into 2 beakers filled with paraffin for 1 h. Finally, they were routinely sectioned and stained with hematoxylin eosin. The stained sections were inspected with a microscope ($200×$ magnification) and were also imaged. Two pulmonary artery samples from 2 normal birds were selected for histopathologic examination and RNA sequencing.

mRNA Data Analysis

The pulmonary artery total RNA was extracted using TRIzol reagent (Invitrogen, Burlington, ON, Canada) as per the manufacturer's protocol. A total of 3 µg RNA per sample was used with sequencing libraries, which were generated using the NEBNext1UltraRNA Library Prep Kit for Illumina1 (NEB) following the manufacturer's recommendations, and the index codes were added to attribute the sequences to each sample. Data analysis has been reported in our previous experiments (Liu et al., 2017). Raw data in FASTQ format in the present study have been deposited in Short Read Archive database of the National Center for Biotechnology Information with an accession number SRP068247.
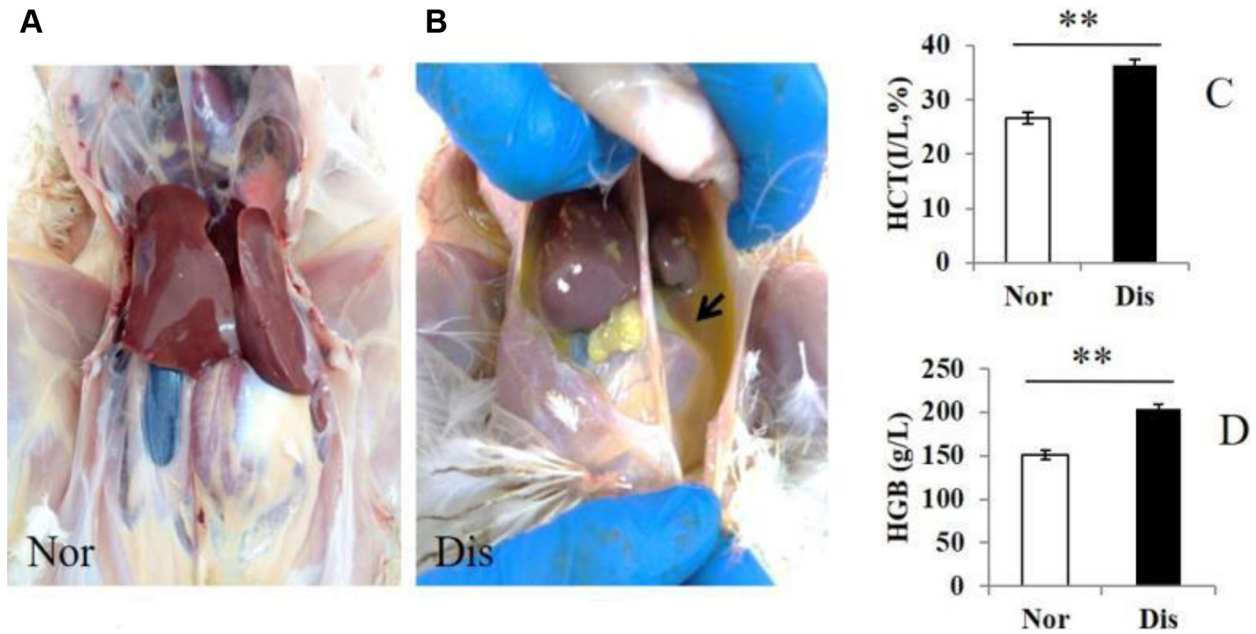
Figure 1. Necropsy changes and analysis of related biochemical indexes. Abbreviations: Dis, disease group; HCT, hematocrit; HGB, hemoglobin; Nor, normal group.

Analysis of SNP

SNP sites of upregulated and downregulated genes were analyzed for the normal group and the disease group of PAH of AS in broilers. Selection of mRNA-related SNP was between the differences of SNP associated with transcriptome data of the 2 groups by selecting 2 groups of samples with homozygous and different SNP. Specifically, the transcriptome mutation detection was conducted in GATK and SNP/InDel correlation were analyzed by ANNOVAR. At the same time, we filtered the SNP and corrected SNP near indel by GATK and screened nonoverlapping exons of SNP (reference reads ≥ 2, mutation reads ≥ 3, and mutation frequency $0.1 \sim 0.9$).
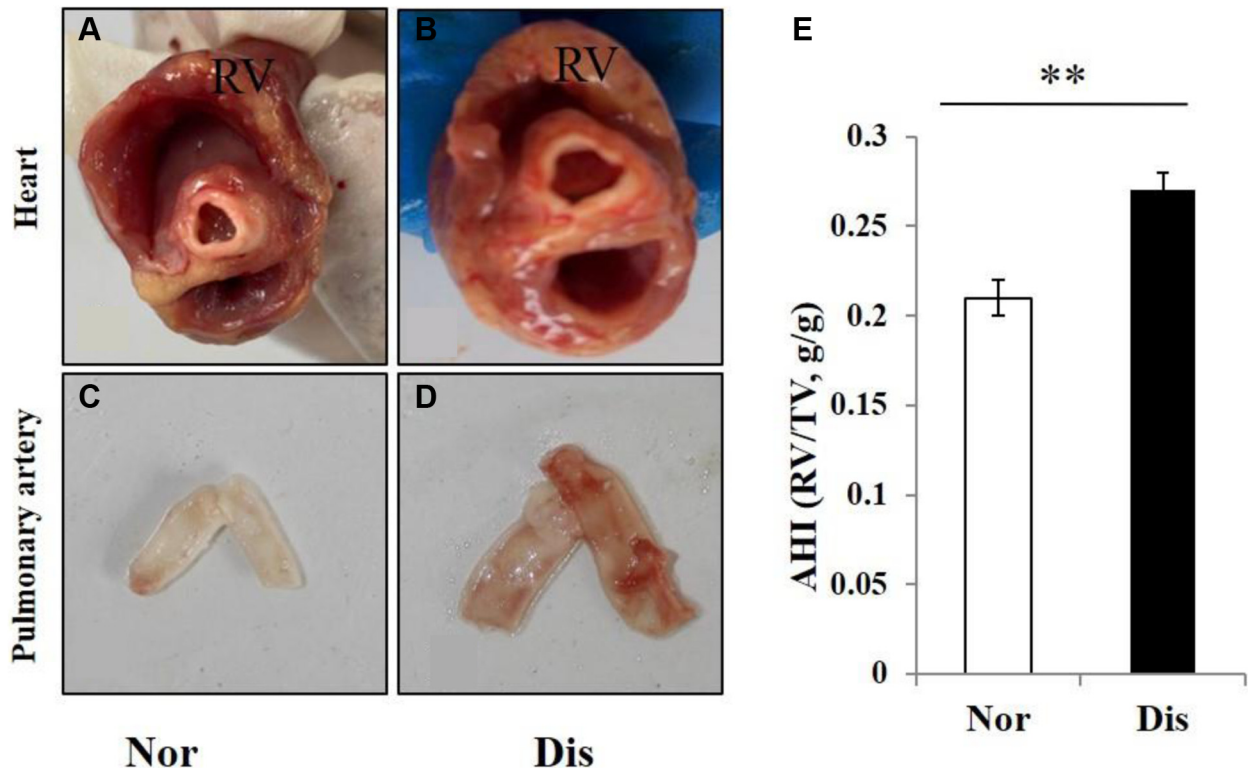

Figure 2. Heart and cardiac index analysis. (A) The normal heart; (B) The heart of the disease group; (C) Healthy pulmonary artery in normal group; (D) pulmonary artery hypertrophy and hemorrhage in disease group; (E) Summary of AHI in disease and normal groups. Abbreviations: Dis, disease group; Nor, normal group; RV/TV, right ventricular weight/total ventricular weight.
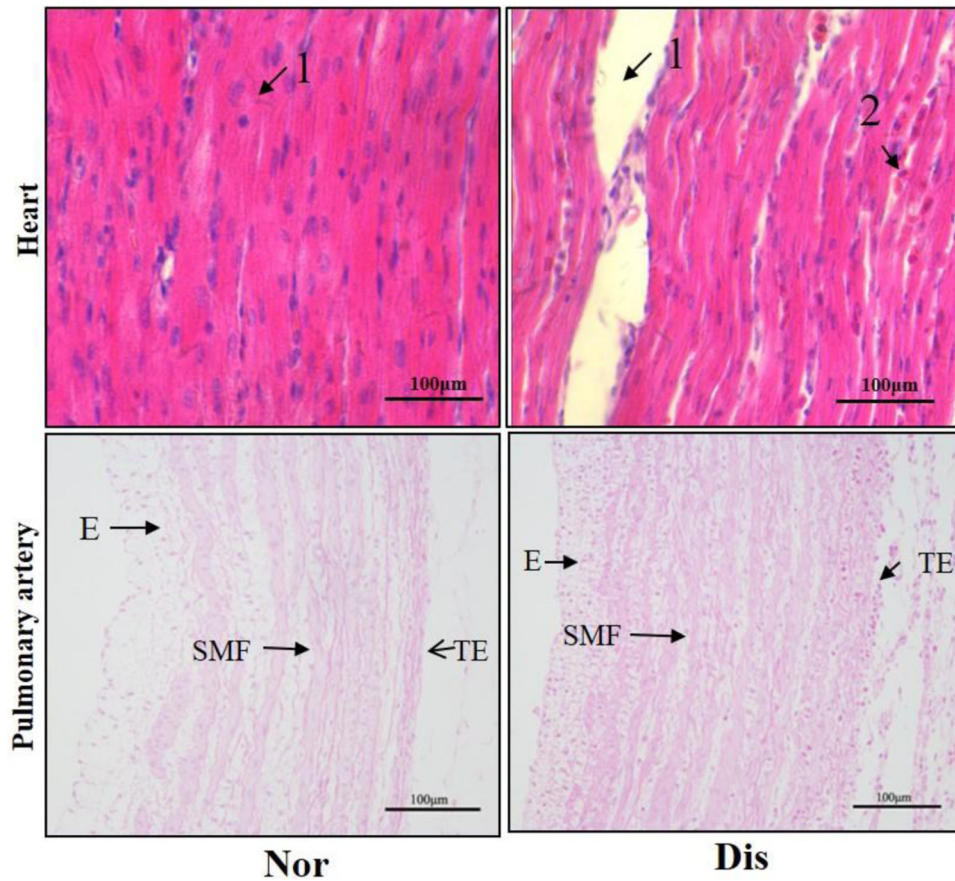
Figure 3. Observation of heart sections: In the D sample, (1) Myocardial cells showed granular degeneration, vacuole degeneration; (2) myocardial fiber rupture and high capillary expansion. Observation of pulmonary artery sections (200X, HE) The wall thickness of disease (D) pulmonary artery is markedly increased. In the D sample, 1) the smooth muscle fiber got thicker; 2) there was excessive fiber production; and 3) the intima was more compact. And, the arrows indicate the pathologic changes. Abbreviations: Dis, disease group; Nor, normal group.

RESULTS

Analysis of Related Indexes of Autopsy

Autopsy and pulmonary artery changes in the normal group and disease group were shown in Figure 1. There were apparent pale yellow liquid and obvious ascites in the abdominal cavity in the broilers with AS. Hemoglobin, AHI, and HCT values indicated that AS was extremely higher in the disease group compared with the normal group. The PH with right ventricular hypertrophy was significantly thicker in the disease group (Figure 2).

Pathologic Changes in the Pulmonary Artery

The heart and pulmonary artery changes on the pathologic level were displayed in Figure 3. It was noticed that granular degeneration of myocardial cells, rupture
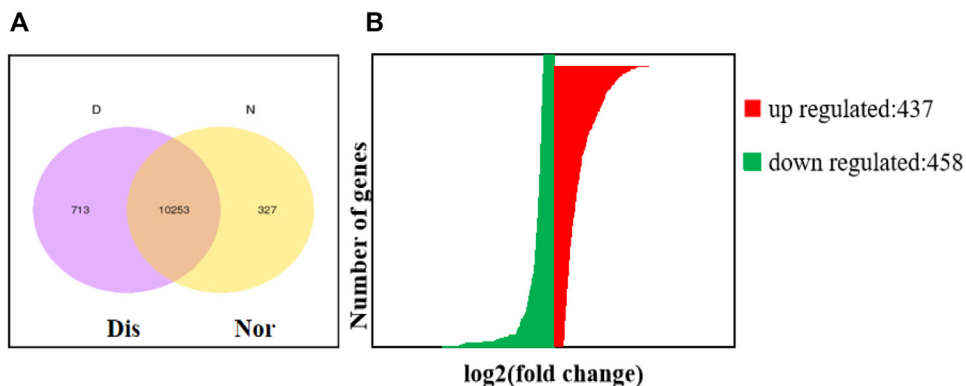

Figure 4. (A) Gene expression profile of disease group and normal group. (B) Volcano diagram displaying differentially expressed genes between the Dis and Nor samples. The significantly upregulated genes are in red and the downregulated genes are in green. Abbreviations: Dis, disease group; Nor, normal group.
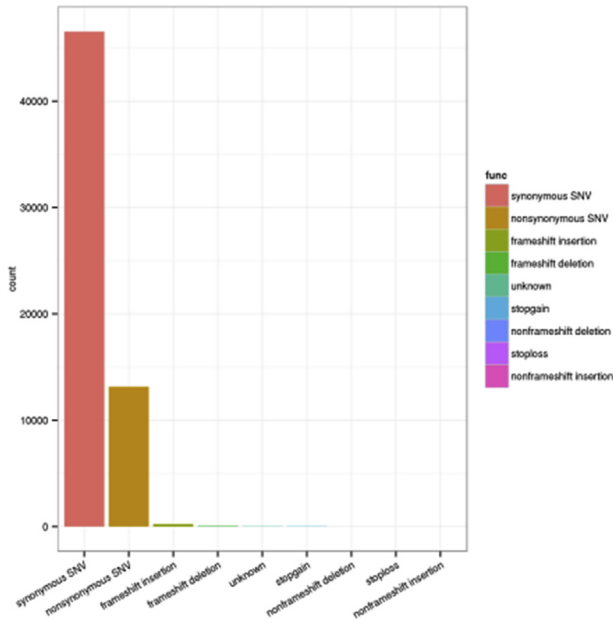
Figure 5. SNP function classification diagram.

of myocardial fibers, and high expansion of capillaries were observed. Meanwhile, the thickness of the pulmonary artery in the AS broilers was markedly elevated, while the medial smooth muscle layers became thicker and were discontinuous and disordered. Moreover, the mesenchyme between the muscular layers was much more loose in the broilers with AS compared with that in the normal broilers.

Differential Expression Analysis

The genes expression density distributions between disease and normal samples were shown. To understand the expression patterns of the differentially expressed genes, we performed hierarchical clustering of those
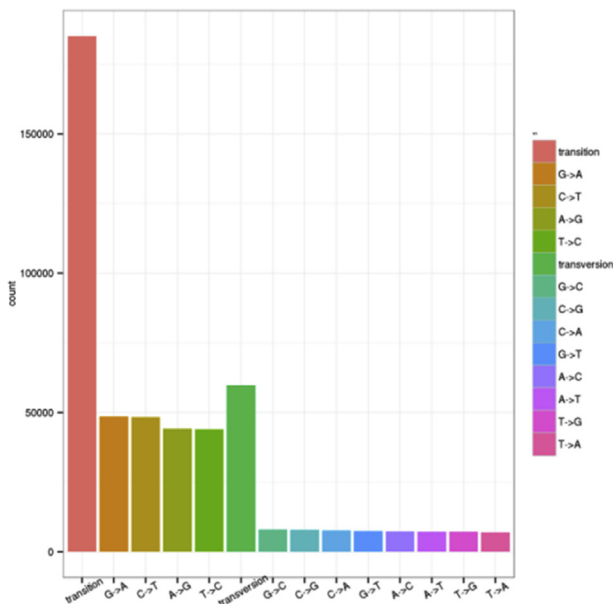

Figure 6. SNP mutation statistics.

differentially expressed genes based on the RPKM values for the genes in the 4 samples. Both disease samples and normal samples had high-expressed and low-expressed genes, implying that the development of AS relies on various mechanisms (Figure 4A). A total of 895 genes that were differentially expressed in the pulmonary arteries between the disease broilers and the normal broilers were identified. Among them, there were 437 upregulated genes and 458 downregulated genes (Figure 4B).

SNP Function Classification

Figure 5 shows the results of mutation detection using GATK software and SNP/InDel correlation using ANNOVAR software based on the transcriptome data. Our SNP data showed that most of the genes had no synonymous mutations, but there were some nonsynonymous mutations, which indicated that some amino acid sequences or functional RNA base sequences were mutated. Nonsynonymous mutations play an important role in evolutionary biology in determining gene positive selection and purifying selection.

The essence of gene mutation is the change in DNA base sequences. DNA substitution mutations are of 2 types. Transitions are interchanges of two-ring purines (A-G) or of one-ring pyrimidines (C-T): they therefore involve bases of similar shape. Transversions are interchanges of purine for pyrimidine bases, which therefore involve exchange of one-ring and two-ring structures. It can be seen from Figure 6 that some genes in a large number of samples have base conversion and transversion, and the proportion of conversion is significantly higher than the proportion of transversion.

We used the difference in SNP of 2 samples and the table of 2 groups of difference genes to merge and get the intersection results. The aim was to find differentially expressed gene, and the results were as follows (Table 1).

DISCUSSION

Many studies demonstrated that mRNA expressions are tissue-specific and cell-specific and can be dysregulated in diseases. More importantly, many mRNA expression levels are correlated with disease severity (Grant et al., 2013; Xu et al., 2016). Many mRNA have been identified as being associated with PAH via high-throughput sequencing (Grant et al., 2013; Li et al., 2014). Sequence analysis showed that the main size of small RNA in the pulmonary arteries in normal chickens and disease chickens is 18–35, and 22 poly-N tags is the predominant size. This result is consistent with the known 19–24 nt range for miRNAs, and previous studies in chicken skeletal muscle, breast muscle tissues, and ovary also demonstrate similar results. Pulmonary arterial hypertension involves pathogenic dysregulation of all cell types within the small pulmonary arteries contributing to vascular remodeling leading to intimal lesions, resulting in elevated pulmonary vascular resistance and right heart dysfunction (Grant et al., 2013). In the present study, the pulmonary

Table 1. Intersection of differential gene and differential SNP.

Associated gene name	GeneID	#Chr	Start	End	Ref	Mut	Quality	Dis_type	Nor_type	Dis_read	Nor_read	Padj
ALDH7A1	ENSGALG00000008229	Z	78,751,037	78,751,037	C	A	1754.42	1|1	0|0	0,41	23,0	0.01793
IRG1	ENSGALG00000016919	1	1.54 E+08	153,687,812	G	A	1335.85	1|1	0|0	0,31	2,0	2.11E-18
GGT5	ENSGALG00000006501	15	8,373,841	8,373,841	G	C	673.17	1|1	0|0	0,16	4,0	2.96E-06
IGSF1	ENSGALG00000000974	20	43,121	43,121	C	T	457.86	1|1	0|0	0,11	2,0	0.00991
DHX58	ENSGALG00000023821	27	4,825,729	4,825,729	G	A	392.86	1|1	0|0	0,10	2,0	1.56E-06
USP36	ENSGALG00000028462	18	10,052,169	10,052,169	G	A	191.67	1|1	0|0	0,5	1,0	0.03729
TREML2	ENSGALG00000023780	26	4,698,355	4,698,355	A	C	187.67	1|1	0|0	0,5	1,0	0.024573
SPAG1	ENSGALG00000016037	2	1.28 E+08	128,193,163	A	G	147.45	1|1	0|0	0,4	3,0	0.014448
SERPING1	ENSGALG00000007381	5	16,310,617	16,310,617	C	T	98.38	1|1	0|0	0,3	1,0	1.58E-05
CD34	ENSGALG00000001177	26	2,674,557	2,674,557	A	G	58.01	1|1	0|0	0,2	18,1	0.004791
PLEKHA7	ENSGALG00000006090	5	11,057,072	11,057,072	A	T	52.93	1|1	0|0	0,2	7,0	0.013052

arteries from AS broilers were collected to investigate the relationship between mRNA and SNP using high-throughput sequencing technology. To correctly identify AS broilers before collecting samples for RNA sequencing, we used common parameters such as yellow liquid accumulation in the abdominal cavity and pericardium, AHI (right ventricular/total ventricular) > 0.249, and increased HCT and hemoglobin levels when compared with normal birds (Wideman et al., 2013; Bai et al., 2014; Babcock et al., 2015). These parameters supported our present results regarding right ventricular/total ventricular and the difference in routine blood indexes, such as HCT and hemoglobin, between the disease group and the control group (Figure 4). As per our previous RNA sequencing analysis in AS pulmonary arteries, there were a total of 895 miRNA detected, with 437 being upregulated and 458 being downregulated (Figure 4). The SNP loci of upregulated and downregulated genes were analyzed to identify the mutant genes, GATK was used for transcriptome mutation detection, and ANNOVAR was used for SNP/InDel correlation analysis.

Mutation is the major source of selection and adaptation (Olkowski, 2007; Wideman et al., 2013). In the coding regions of DNA, it is expected that the nonsynonymous mutations that change the protein sequences would undergo strong selection, and those nonsense mutations that cause premature termination of protein synthesis are also highly deleterious and subject to purifying selection. However, the selection on synonymous mutations for a long time was thought to be negligible or very weak (Chu and Wei, 2019). In this study, it was shown that mutant genes promoted the pulmonary artery remodeling and contributed to PH occurrence. In this present experiment, we found the following mutated genes: ALDH7A1, IRG1, GGT5, IGSF1, DHX58, USP36, TREML2, SPAG1, CD34, PLEKHA7. In the present study, we observed that ALDH7A1 plays a key role in the pulmonary artery remodeling and vascular contraction, and they all contributed to the occurrence of AS by elevating vascular resistance. ALDH7A1 knockdown has been shown to cause reduced cell proliferation in the optic cup of the zebrafish (Babcock et al., 2014) and function degradation in lipid peroxidation in chickens (Bai et al., 2014). Cell proliferation are closely linked to pulmonary

artery remodeling. Thus, this suggests that ALDH7A1 could serve as a potential gene target for preventing AS progression. Immune responsive gene 1 (**IRG1**) is referred to as a positive transcription factor as it induces several genes, which are important in regulating several immunologic and physiological functions in mammalian cells. Immune responsive gene 1 is also transcriptionally activated by several proinflammatory cytokines and pathogens. In addition, IRG1 is one of the highest expressed induced genes in macrophages under proinflammatory conditions. Therefore, IRG1 in inflammation could contribute to pulmonary artery remodeling, activating the development of PH. Previous studies have shown that in the mouse, macrophages under proinflammatory conditions, such as bacterial infections or lipopolysaccharide stimulation, there are high expression in IRG1 (Tallam et al., 2016), which is consistent with our results. Gamma-glutamyl transferase 5 is a key metabolism component responsible for the catalysis of important antioxidant glutathione. Gamma-glutamyl transferase 5 and its substrates probably play more important roles under certain types of pathologic stress, which is interesting and warrants further investigation (Li et al., 2016). Ig superfamily member 1 (**IGSF1**) and c58 were found to be associated with the "immune response" and be involved in cellular antiviral immunity by affecting the immunity-related genes. The IGSF1) gene encodes a plasma membrane glycoprotein, which causes different symptoms. Meanwhile, it was reported that DHX58 was significantly dysregulated by herpes simplex virus 1 infection (Shi et al., 2018). Loss-of-function analysis showed that IGSF1 and DHX58 knockdown could inhibit cell proliferation, leading to vascular dysfunction and a loss of vascular integrity via the regulation of the proliferation, migration, and survival of smooth muscle cells in mice (Li et al., 2010; Guan et al., 2019; Hebbar et al., 2020). This report supports our finding that IGSF1 and DHX58 gene mutations are involved in pulmonary arteries during AS progression. USP36 has been implicated in the regulation of nucleolar activity, which is a nucleolar protein related to ribosome biogenesis and RNA processing regulation. USP36-deficient morulae exhibit impaired protein synthesis, highlighting the importance of USP36 in this cellular process (Li et al., 2010; Guan et al., 2019; Hebbar et al., 2020). Moreover, northern blot analysis

has shown that USP36 deficiency induces aberrations in rRNA synthesis and apoptosis at the preimplantation stage of development (Fraile et al., 2018). Whole-exome sequencing data identified a coding missense variant (rs3747742-C) in triggering receptor expressed on myeloid cells-like 2 (**TREML2**) gene. The variant rs3747742-C results in an amino acids substitution at residue144 of TREML2, which was expected to affect the biological functions of this protein. Triggering receptor expressed on myeloid cells-like 2 was revealed to be upregulated in microglia and astrocytes after inflammatory stimulation and might amplify inflammatory responses during disease progression (Jiang et al., 2017). Similar effect was found in IRG1, which plays an important role in pathologic sections. Mutations in SPAG1 causes primary ciliary dyskinesia associated with defective outer and inner dynein arms. Zebrafish morpholino studies of SPAG1 produced cilia-related phenotypes, which was previously reported for primary ciliary dyskinesia causing mutations in genes encoding cytoplasmic proteins, and the structural change of protein caused by the mutation of SPAG1 gene directly affects the function of organism. Hereditary vascular edema is an autosomal dominant disease characterized of recurrent edema attacks associated with morbidity and mortality. Hereditary vascular edema results from variations in the SERPING1 gene that provides instructions for making a protein called C1 inhibitor, which is a type of serine protease inhibitor (**serpin**). C1 inhibitor is important for controlling a range of processes involved in maintaining blood vessels, including inflammation. The changes in SERPING1 gene have a direct response to infection, irritation, and other injury on ascites in broilers (Calvo-Ferrer et al., 2019). CD34, a membrane glycoprotein, is a critical component of the group of surface receptors that regulate migration and engraftment of progenitor cells to target tissues. $CD34^+$ endothelial progenitor cells play an important role in the recovery of the injured. Some studies found an increase in resident CD34-positive cells in the aortic tissue of humans and mice during ATH progression, as well as the presence of clusters of CD34-positive cells in the intima and adventitia of human ATH aortas (Hueso et al., 2019; Zhang et al., 2019). PLEKHA7 was found to play a significant role in hypertension,and it had complex risk of other SNP and would gradually increase the risk of hypertension. This discovery is in good agreement with our experimental result. Hence, these present results may implicate that these miRNA changes will result in changes of vessel wall and the function barrier in PAH by affecting some target genes at post-transcriptome level. In summary, those target genes of miRNA found in this study may promote the pulmonary artery remodeling by being involved in inflammation and proliferation.

In the present study, the pathologic examination found the pulmonary artery remodeling characterized of thickening of the artery wall, especially in the medial intima consisting of vascular smooth muscle cells (Figure 2). Previous pathologic studies also reported similar characteristics of pulmonary artery remodeling in AS broilers, which resulted from hypertrophy, proliferation, and sparse migration of the affected cell (Qiao et al., 2012). Pulmonary vascular remodeling was confirmed as an important pathologic contributor to AS that leads to an increase in pulmonary vascular resistance, prolonging elevated arterial hypertension (Lin et al., 2017). Among vascular well cells, the proliferation and hypertrophy of vascular smooth muscle cells were thought to be a main contributor that facilitates pulmonary vascular remodeling and has an important role in AS progression (Wang et al., 2007), which was in accordance with the reported changes in this study.

In addition, the pathologic observation further demonstrated that the current findings of differentially expressed mRNA and correlated targets in the pulmonary arteries from broilers with AS maybe the main molecular regulators for pulmonary artery remodeling.

CONCLUSION

The present study revealed specific potential pathways of the complex molecular circuitry in AS broilers such as mutant genes, including ALDH7A1, IRG1, GGT5, IGSF1, DHX58, USP36, TREML2, SPAG1, CD34 and PLEKHA7. Our study found the mutant genes, which further demonstrate that revealed target genes and pathways in this study are meaningful for the prevention of PAH in both humans and broilers in the future.

ACKNOWLEDGMENTS

DISCLOSURES

The authors declare no conflicts of interest.

REFERENCES

Babcock, H. E., S. Dutta, R. P. Alur, C. Brocker, V. Vasiliou, S. Vitale, M. Abu-Asab, and B. P. Brooks. 2014. aldh7a1 regulates eye and limb development in zebrafish. PLoS One 9:e101782.

Baghbanzadeh, A., and E. Decuypere. 2008. Ascites syndrome in broilers: physiological and nutritional perspectives. Avian Pathol. 37:117–126.

Bai, H., J. Zhu, Y. Sun, R. Liu, N. Liu, D. Li, J. Wen, and J. Chen. 2014. Identification of genes related to beak deformity of chickens using digital gene expression profiling. PLoS One 9:e107050.

Calvo-Ferrer, M., S. Martín-Rodríguez, N. Ortega-Unanue, Á. Blasco-Sarramián, and I. Bernardo-González. 2019. A novel SERPING1 gene variant causing angioedema in a patient with low C1q levels. Ann. Allergy Asthma Immunol. 123:610–612.

Chu, D., and L. Wei. 2019. Nonsynonymous, synonymous and nonsense mutations in human cancer-related genes undergo stronger purifying selections than expectation. BMC Cancer 19:312–359.

Fraile, J. M., D. Campos-Iglesias, F. Rodríguez, A. Astudillo, R. Vilarrasa-Blasi, N. Verdaguer-Dot, M. A. Prado, J. A. Paulo, S. P. Gygi, J. I. Martín-Subero, J. M. P. Freije, and C. López-Otín. 2018. Loss of the deubiquitinase USP36 destabilizes the RNA helicase DHX33 and causes preimplantation lethality in mice. J. Biol. Chem. 293:2183–2194.

Grant, J. S., K. White, M. R. MacLean, and A. H. Baker. 2013. MicroRNAs in pulmonary arterial remodeling. Cell. Mol. Life Sci. 70:4479–4494.

Guan, Y., Y. Wang, A. Bhandari, E. Xia, and O. Wang. 2019. IGSF1: a novel oncogene regulates the thyroid cancer progression. Cell Biochem. Funct. 37:516–524.

Hebbar, P., M. Abu-Farha, F. Alkayal, R. Nizam, N. Elkum, M. Melhem, S. E. John, A. Channanath, J. Abubaker, A. Bennakhi, E. Al-Ozairi, J. Tuomilehto, J. Pitkaniemi, O. Alsmadi, F. Al-Mulla, and T. A. Thanaraj. 2020. Genome-wide association study identifies novel risk variants from RPS6KA1, CADPS, VARS, and DHX58 for fasting plasma glucose in Arab population. Sci. Rep. 10:152.

Hueso, M., J. M. Cruzado, J. Torras, and E. Navarro. 2019. An exonic Switch regulates differential accession of microRNAs to the Cd34 transcript in atherosclerosis progression. Genes (Basel) 10:7.

Jiang, T., Y. Wan, J. Zhou, M. Tan, Q. Huang, X. Zhu, H. Lu, H. Wang, Q. Chen, L. Tan, Y. Zhang, L. Tan, and J. Yu. 2017. A missense variant in TREML2 reduces risk of Alzheimer's disease in a han Chinese population. Mol. Neurobiol. 54:977–982.

Julian, R. J. 2000. Physiological, management and environmental triggers of the ascites syndrome: a review. Avian Pathol. 29:519–527.

Li, X. Y., C. M. Han, Y. Wang, H. Z. Liu, Z. F. Wu, Q. H. Gao, and S. H. Zhao. 2010. Expression patterns and association analysis of the porcine DHX58 gene. Anim. Genet. 41:537–540.

Li, S., Y. Ran, D. Zhang, S. Li, and D. Zhu. 2014. MicroRNA-190 regulates hypoxic pulmonary vasoconstriction by targeting a voltage-gated K+ channel in arterial smooth muscle cells. J. Cell. Biochem. 115:1196–1205.

Li, W., Z. Q. Wu, S. Zhang, R. Cao, J. Zhao, Z. J. Sun, and W. Zou. 2016. Augmented expression of gamma-glutamyl transferase 5 (GGT5) impairs testicular steroidogenesis by deregulating local oxidative stress. Cell Tissue Res. 366:467–481.

Liu, P., F. Yang, Y. Zhuang, Q. Xiao, H. Cao, C. Zhang, T. Wang, H. Lin, X. Guo, and G. Hu. 2017. Dysregulated expression of microRNAs and mRNAs in pulmonary artery remodeling in ascites syndrome in broiler chickens. Oncotarget 8:1993–2007.

Mullany, L. E., R. K. Wolff, J. S. Herrick, M. F. Buas, and M. L. Slattery. 2015. SNP regulation of microRNA expression and subsequent colon cancer risk. PLoS One 10:e143894.

Olkowski, A. A. 2007. Pathophysiology of heart failure in broiler chickens: structural, biochemical, and molecular characteristics. Poult. Sci. 86:999–1005.

Papamatheakis, D. G., A. B. Blood, J. H. Kim, and S. M. Wilson. 2013. Antenatal hypoxia and pulmonary vascular function and remodeling. Curr. Vasc. Pharmacol. 11:616–640.

Qiao, L., L. Xie, K. Shi, T. Zhou, Y. Hua, and H. Liu. 2012. Notch signaling change in pulmonary vascular remodeling in rats with pulmonary hypertension and its implication for therapeutic intervention. PLoS One 7:e51514.

Schermuly, R., B. Dahal, S. Pullamsetti, H. Ghofrani, W. Seeger, R. Heuchel, J. Wilhelm, N. Weissmann, and F. Grimminger. 2011. Hypoxic pulmonary hypertension in mice with constitutively active platelet-derived growth factor receptor-β. Pulm. Circ. 1:259.

Shi, J., N. Hu, L. Mo, Z. Zeng, J. Sun, and Y. Hu. 2018. Deep RNA sequencing reveals a repertoire of human fibroblast circular RNAs associated with cellular responses to herpes simplex virus 1 infection. Cell. Physiol. Biochem. 47:2031–2045.

Shimoda, L. A., and S. S. Laurie. 2013. Vascular remodeling in pulmonary hypertension. J. Mol. Med. 91:297–309.

Tallam, A., T. M. Perumal, P. M. Antony, C. Jäger, J. V. Fritz, L. Vallar, R. Balling, A. Del Sol, and A. Michelucci. 2016. Gene regulatory network inference of immunoresponsive gene 1 (IRG1) identifies interferon regulatory factor 1 (IRF1) as its transcriptional regulator in mammalian macrophages. PLoS One. 11:e149050.

Wang, J., J. Qiao, L. H. Zhao, K. Li, H. Wang, T. Xu, Y. Tian, M. Gao, and X. Wang. 2007. Proliferation of pulmonary artery smooth muscle cells in the development of ascites syndrome in broilers induced by low ambient temperature. J. Vet. Med. A. Physiol. Pathol. Clin. Med. 54:564–570.

Wideman, R. F., D. D. Rhoads, G. F. Erf, and N. B. Anthony. 2013. Pulmonary arterial hypertension (ascites syndrome) in broilers: a review. Poult. Sci. 92:64–83.

Xu, T., Q. Zhou, L. Che, S. Das, L. Wang, J. Jiang, G. Li, J. Xu, J. Yao, H. Wang, Y. Dai, and J. Xiao. 2016. Circulating miR-21, miR-378, and miR-940 increase in response to an acute exhaustive exercise in chronic heart failure patients. Oncotarget 7:12414–12425.

Zhang, H., Y. Wang, Y. Tan, H. Wang, P. Tao, and P. Zhou. 2019. Enhancement of cardiac lymphangiogenesis by transplantation of CD34+VEGFR-3+ endothelial progenitor cells and sustained release of VEGF-C. Basic Res. Cardiol. 114:43.